(Received 23 April 2025, Accepted 16 June 2025, Scheduled 27 June 2025)

Study on Deployment Scheme of 5G Communication Devices in Complex Electromagnetic Environment of Substations

Hanhan Hu, Jieqing Fan*, Rui Zhu, and Zhaomin Han

North China Electric Power University, Beijing 102206, China

ABSTRACT: Addressing the deployment challenges of 5G communication equipment in the complex electromagnetic environment of substations, this paper takes an actual substation as the research object. Through a combined approach of physical modeling and field measurement validation, it systematically investigates the deployment issues of 5G devices in substations. Firstly, a power frequency electromagnetic field model of the substation is established, and its reliability is verified by comparative analysis between simulation results and on-site measured data. Secondly, by establishing a radiation model of 5G communication equipment, the mutual interference between 5G devices and secondary equipment within the substation is investigated. Finally, leveraging the distribution characteristics of the power frequency electromagnetic field in the substation, a tailored deployment scheme for 5G communication equipment is proposed. This study provides both a theoretical foundation and technical support for the practical deployment of 5G in smart substations, thereby advancing the deep integration of power systems and communication systems.

1. INTRODUCTION

With the deep integration of 5G communication technology and smart grid, smart substations are accelerating their evolution into the core nodes of power system [1]. As the core facility of a power system, substations are crucial locations where high-voltage and low-voltage electricity is highly concentrated. The main sources of interference to communication equipment from the complex electromagnetic environment inside the substation are steady-state electromagnetic environment and transient electromagnetic environment. Among them, steady-state electromagnetic environment is particularly critical, as it consists of power frequency electric fields, power frequency magnetic fields during normal substation operation, and intrinsic electromagnetic interference from secondary equipment. It is characterized by strong persistence and wide-ranging influence. In particular, high-intensity power frequency electromagnetic fields and electromagnetic interference (EMI) generated by various power equipment can significantly degrade the electromagnetic compatibility (EMC) performance of 5G communication devices, posing severe technical challenges for the deployment of 5G base stations. In contrast, transient electromagnetic environments, such as rapid transient pulse groups caused by switch operations or lightning surges, although characterized by transient high-energy features, typically have sporadic effects [2]. Therefore, the long-term cumulative effects of steady-state electromagnetic environments pose a more serious challenge to the electromagnetic compatibility performance of 5G base stations, becoming a key factor restricting the reliable deployment of 5G communication equipment in substation scenarios.

At present, research has not yet formed a systematic theoretical and methodological system for the deployment of 5G communication equipment in the complex electromagnetic environment of substations. Existing research mainly focuses on the following three aspects: (1) Existing literature indicates that the power frequency electromagnetic field intensity at most measurement points in high voltage substations exceeds the national occupational exposure limit values. The power frequency electromagnetic interference generated by power equipment such as transmission lines in normal operating conditions significantly impacts the deployment of communication equipment [3–5]. (2) The equipment within a substation is complex and numerous. Existing research primarily focuses on partial models of substations, while comprehensive numerical simulations of power frequency electromagnetic fields across the entire transmission lines in substations remain relatively scarce [6, 7]. (3) In the field of electromagnetic compatibility research, existing achievements primarily focus on electromagnetic interference issues among traditional equipment within substations [8, 9]. However, research on the mutual interference between 5G communication devices and secondary equipment within substations remains scarce, with most existing studies confined to experimental testing phases. Investigating the mutual interference between 5G communication devices and secondary equipment is critical for evaluating their electromagnetic compatibility, ensuring reliable operation, and mitigating potential disruptions. With the rapid advancement of 5G communication technology and its expanding application scope, growing attention is paid to its potential deployment in complex environments like substations. Therefore, it is urgent to conduct the research on the deployment of 5G communication equipment in complex electromagnetic environments within substations. To this end,

* Corresponding author: Jieqing Fan (fanjieqing@ncepu.edu.cn).

this paper mainly discusses the mutual influence between 5G communication equipment and secondary equipment under the complex electromagnetic environment, as well as the impact of the long-term stable existence of industrial frequency electromagnetic fields in the substation on the deployment of 5G communication equipment. Finally, this study proposes a deployment scheme for 5G communication equipment in substations, providing both theoretical foundations and technical support for practical implementation within smart substation environments.

2. PRINCIPLES OF POWER FREQUENCY ELECTROMAGNETIC FIELD CALCULATION IN TRANSMISSION LINES

The substation contains a diverse array of irregularly distributed excitation sources. Furthermore, electromagnetic interactions between energized conductors, insulators, and grounding structures generate an exceptionally complex field environment. This complexity poses significant challenges for accurate numerical modeling using conventional computational methods [10]. To address this, the present study proposes a computational model for power frequency electromagnetic fields in substations under three-phase transmission lines with sag consideration. This model integrates the Method of Simulated Charges and the Method of Moments, building upon traditional numerical electromagnetic field calculation methods to enhance the accuracy and reliability of results.

2.1. Power Frequency Electric Field

For electromagnetic field calculations involving bundled conductors in high-voltage transmission lines (≥ 110 kV), the subconductors of each phase may be equivalently modeled as a single composite conductor. Assuming that the n subconductors of a bundled conductor are uniformly arranged in a circular configuration, the equivalent radius of the conductor can be expressed by Equation (1).

$$R_{eq} = R\sqrt[n]{\frac{nr}{r}} \tag{1}$$

In the equation: R_{eq} is the equivalent radius of the composite conductor; R is the radius of the circular bundle formed by the subconductors; n denotes the number of subconductors; r is the individual radius of each subconductor.

Assuming that the transmission lines within one span are arranged in a catenary distribution, the suspension points at both ends of the conductor are at the same height horizontally. The spacing between the conductors of the three-phase transmission line is equal and denoted as L. The highest point has a height of H, and the sag is denoted as S. In space, at a certain point with coordinates $M(x, y, z)$, taking the conductor of phase B of the three-phase transmission line directly below as the origin, with the direction of the transmission line as the x-axis direction, the vertical direction as the y-axis direction, and the direction perpendicular to the ground as the z-axis direction, the schematic diagram of the overhead catenary line is established as shown in Figure 1.

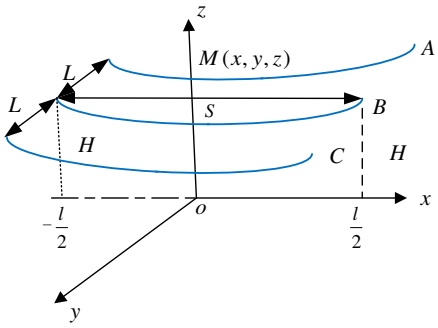

FIGURE 1. Schematic diagram of the overhead catenary line.

The general equation of the catenary line of the transmission line is shown as Equation (2).

$$\begin{aligned} \mathrm{Z} =& \frac{L}{\alpha}\left(\cosh\frac{\alpha(x-kL)}{L} - \cosh\frac{\alpha}{2}\right) + H, \\ & -\frac{L}{2} \leq x - kL \leq \frac{L}{2} \end{aligned} \tag{2}$$

In the equation: L represents the span length; $\alpha = \frac{\gamma L}{\sigma_0}$ denotes the horizontal stress coefficient of the conductor; γ is the specific load of the conductor, combining weight and external loads; σ_0 indicates the horizontal stress applied to the conductor.

The electric potential generated in space by the equivalent charges of phase n conductor l_n and its mirror image l'_n is expressed as:

$$\vec{\varphi}_n = \frac{1}{4\pi\varepsilon_0}\int_{l_n}\left(\frac{1}{r_n} - \frac{1}{r'_n}\right)\mathrm{d}l'_n \tag{3}$$

In the equation: ε_0 represents the vacuum permittivity; r_n and r'_n are the spatial distances from the source point (x_n, y_n, z_n) and the mirror point $(x_n, y_n, -z_n)$ to $M(x, y, z)$.

$$r_n = \sqrt{(x-x_n)^2 + (y-y_n)^2 + (z-z_n)^2} \tag{4}$$

$$r'_n = \sqrt{(x-x_n)^2 + (y-y_n)^2 + (z+z_n)^2} \tag{5}$$

As shown in Equation (6):

$$\mathrm{d}l_n = \cosh\frac{\alpha(x_n - kL)}{L}\mathrm{d}x_n \tag{6}$$

Assume that the charge on the conductor in each span is evenly divided into M equal parts, and the linear charge density of each part is $\vec{\tau}_{n(m)}$. In approximate calculation, the space potential can be calculated by taking the continuous $2K+1$ span length transmission line near point M. Then, the potential formed by the n phase conductor at point $M(x, y, z)$ is:

$$\begin{aligned} \vec{\varphi}_n =& \frac{1}{4\pi\varepsilon_0}\sum_{k=-K}^{K}\sum_{m=1}^{K}\left(\vec{\tau}_{n(m)}\int_{\left(k-\frac{1}{2}\right)L+(m-1)\Delta x}^{\left(k-\frac{1}{2}\right)L+m\Delta x}\right. \\ & \left.\left(\frac{1}{\rho_n} - \frac{1}{\rho_{n'}}\right)\cosh\frac{\alpha(x_n - kL)}{L}\mathrm{d}x_n\right) \end{aligned} \tag{7}$$

In this equation:

$$\rho_n = \left((x - x_n)^2 + (y - y_n)^2 + \left\{ z - \frac{L}{\alpha} \left[\cosh \frac{\alpha (x_n - kL)}{L} - \cosh \frac{\alpha}{2} \right] - H \right\}^2 \right)^{1/2} \quad (8)$$

$$\rho_n = \left((x - x_n)^2 + (y - y_n)^2 + \left\{ z + \frac{L}{\alpha} \left[\cosh \frac{\alpha (x_n - kL)}{L} - \cosh \frac{\alpha}{2} \right] - H \right\}^2 \right)^{1/2} \quad (9)$$

According to the superposition principle [11], the total electric potential at point M generated by all transmission line conductors is expressed in Equation (10) as:

$$\vec{\varphi} = \sum_{n=1}^{N} \vec{\varphi}_n \quad (10)$$

The electric field intensity at point M is given by Equation (11) as follows:

$$\begin{aligned} \vec{E} &= -\nabla \vec{\varphi} \\ &= -\left(\frac{\partial \vec{\varphi}}{\partial x} \mathbf{e}_x + \frac{\partial \vec{\varphi}}{\partial y} \mathbf{e}_y + \frac{\partial \vec{\varphi}}{\partial z} \mathbf{e}_z \right) \\ &= \vec{E}_x \mathbf{e}_x + \vec{E}_y \mathbf{e}_y + \vec{E}_z \mathbf{e}_z \end{aligned} \quad (11)$$

In the equation: $\vec{E}_x, \vec{E}_y, \vec{E}_z$ represent the electric field vector components along the x, y, z axes; $\mathbf{e}_x, \mathbf{e}_y, \mathbf{e}_z$ denote the unit vectors corresponding to x, y, z axes.

The root-mean-square value of the electric field intensity at point M is given by Equation (12) as follows:

$$|\mathbf{E}| = \sqrt{\vec{E}_x \vec{E}_x^* + \vec{E}_y \vec{E}_y^* + \vec{E}_z \vec{E}_z^*} \quad (12)$$

In the equation, $\vec{E}_x^*, \vec{E}_y^*, \vec{E}_z^*$ represents the complex conjugate of $\vec{E}_x, \vec{E}_y, \vec{E}_z$.

2.2. Power Frequency Magnetic Field

According to the Biot-Savart Law [12], the magnetic field intensity generated at spatial point $M(x, y, z)$ by the current element dl_n on the n phase transmission line and its mirror image dl'_n is expressed in Equation (13).

$$\mathrm{d}\vec{B}_n = \frac{\mu_0 \vec{I}_n}{4\pi} \left(\frac{r_n \mathrm{d}l_n}{r_n^3} - \frac{r'_n \mathrm{d}l'_n}{r'^3_n} \right) \quad (13)$$

In the equation: μ_0 is the vacuum permeability; $\vec{I}_n$ is the phasor current of the nth phase transmission line; $\alpha = \sqrt{2}\delta \mathrm{e}^{-\mathrm{j}\pi/4}$ is the depth of the ground mirror current, where $\delta = 503\sqrt{\rho/f}$, ρ is the ground resistivity in $\Omega \cdot m$, and f is the power frequency in Hz. For the nth conductor, considering $2K+1$ spans for each phase, the calculation of the magnetic induction vector generated at a certain point by each phase can be obtained by the superposition principle as follows:

$$\vec{B} = \vec{B}_x e_x + \vec{B}_y e_y + \vec{B}_z e_z \quad (14)$$

In the equation: $\vec{B}_x, \vec{B}_y, \vec{B}_z$ represent the magnetic field vector components along the three orthogonal coordinate axes.

The root-mean-square value of the magnetic flux density at the target point is calculated using the composite parabolic numerical integration method, as expressed in Equation (15).

$$|\mathbf{B}| = \sqrt{\vec{B}_x \vec{B}_x^* + \vec{B}_y \vec{B}_y^* + \vec{B}_z \vec{B}_z^*} \quad (15)$$

In the equation, $\vec{B}_x^*, \vec{B}_y^*, \vec{B}_z^*$ represent the complex conjugate of $\vec{B}_x, \vec{B}_y, \vec{B}_z$.

3. POWER FREQUENCY ELECTROMAGNETIC FIELD MODEL

Substations contain diverse equipment capable of generating electric and magnetic field emissions. However, primary and secondary devices are typically housed in metallic shielding enclosures with proper grounding, which effectively blocks electric field radiation. Unlike substation equipment, transmission lines operate without electromagnetic shielding, resulting in substantially stronger field emissions. These unmitigated fields pose significant interference risks to 5G communication systems. Given that the spatial dimensions of a substation are significantly larger than those of bushings and other equipment, by equivalently modeling all lines, bushings, and other components as exposed metallic conductors in air, the resulting simulation can be considered to represent the worst-case electromagnetic environment. Based on the principles of calculation of power frequency electromagnetic fields, a simulation model of the transmission lines is established using an actual substation of the Southern Power Grid as an example, to determine the power frequency electromagnetic field distribution within the substation. The overall layout of the substation is illustrated in Figure 2.

As shown in Figure 2, this smart substation adopts a three-tier voltage hierarchical architecture (110 kV/220 kV/500 kV). The 220 kV and 500 kV equipment areas are each equipped with three high-capacity interconnecting transformers, forming a dual-layer power exchange hub for the regional grid. The converter transformer system enables the high-voltage direct current transmission interface, while the reactive power compensation transformer system provides dynamic reactive power support. The control system, centered around the main control room, integrates a next-generation monitoring platform and deploys multi-band 5G communication base stations to ensure reliable connectivity for digital applications such as intelligent inspection and equipment condition monitoring.

Based on Figure 2 (Overall layout diagram of the substation) and referencing the actual engineering drawings of the substation, a simulation model of the substation's transmission lines

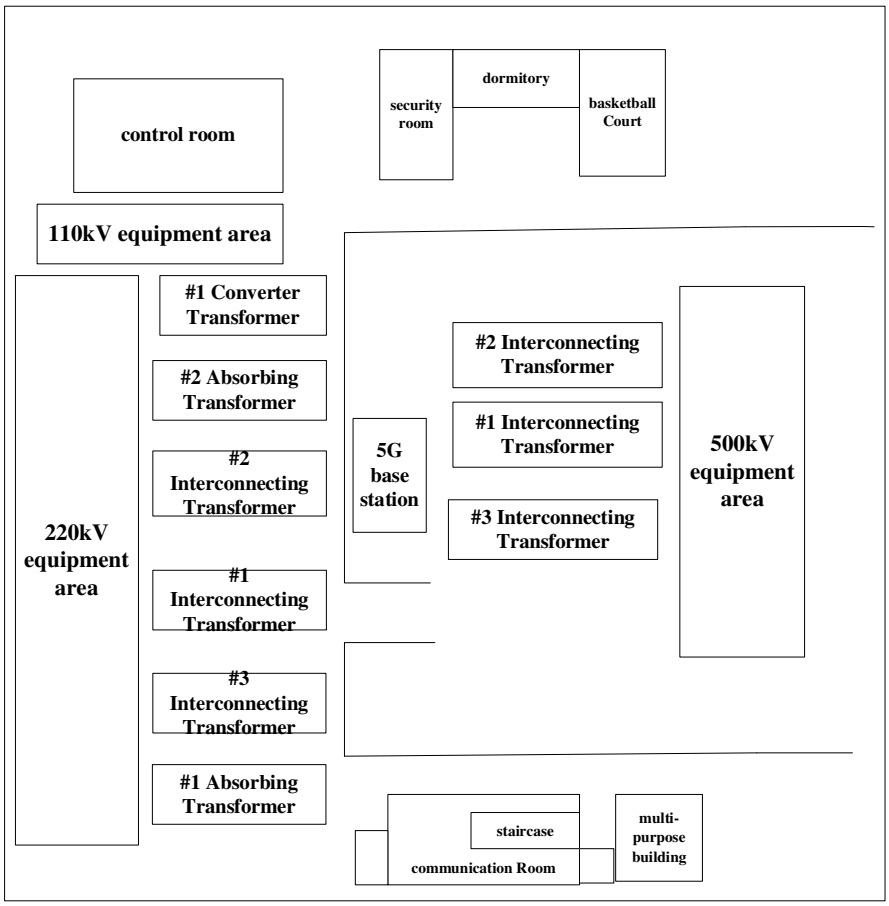

FIGURE 2. Overall layout diagram of the substation.

TABLE 1. Reasonable transmission power of power lines at various voltage levels.

voltage/kV	ground voltage/kV	transmission power /kW	line current/A
35	21.2176	2000–10000	32.99144–164.9572
66	40.0104	3500–30000	30.61706–262.4319
110	66.6839	10000–50000	52.48639–262.4319
220	133.3680	100000–150000	262.4319–393.6479
330	154.9595	400000–600000	699.8185–1049.72
500	303.1089	600000–1000000	692.8203–1154.701

has been developed, as illustrated in Figure 3. The minimum height of the 110 kV transmission line is approximately 3.458 meters, while its maximum height reaches about 7.953 meters. For the 220 kV transmission line, the minimum and maximum heights are 7.4076 meters and 19.7793 meters, respectively. The 500 kV transmission line has a minimum height of 10.862 meters and a maximum height of 21.633 meters. Within the substation, the span between conductors is set at 8 meters.

When simulating transmission lines, it is common to assume that the phase voltages of the transmission lines change according to the three-phase symmetrical sinusoidal law. To better account for actual operating conditions, phase-to-ground voltages of each conductor are typically adopted as simulation inputs to enhance the engineering practicality of results. The phase-to-ground voltage is conventionally set at 1.05 times the phase voltage, thereby covering maximum operational scenarios. The phase-to-ground voltages of each transmission line are shown in Table 1. Therefore, in the simulation, phase-to-ground voltages were applied to one end of the transmission lines with amplitudes of 66.6839 kV for the 110 kV line, 154.9595 kV for the 220 kV line, and 303.1089 kV for the 500 kV line, at phase angles of 0 degrees, -120 degrees, and $+120$ degrees, respectively. This configuration models the 50 Hz power frequency electric field generated by the substation's three-phase power lines under maximum operating conditions.

As indicated in Table 1, the line currents of each transmission circuit are specified. To more accurately simulate the actual operating conditions of the substation, the calculation of

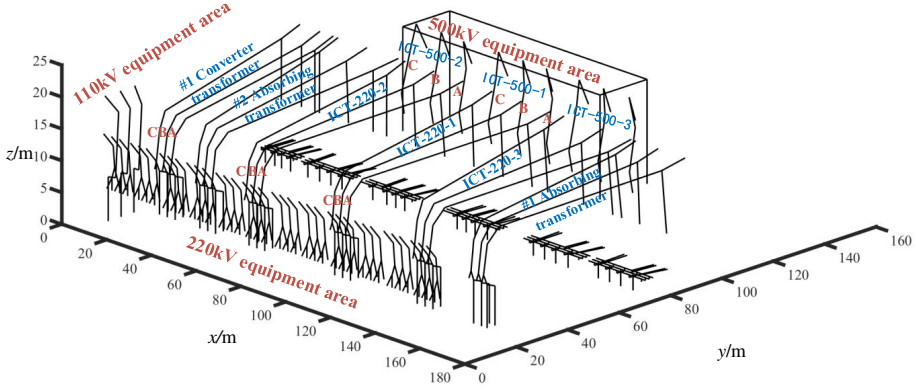

FIGURE 3. Power frequency electromagnetic field simulation model.

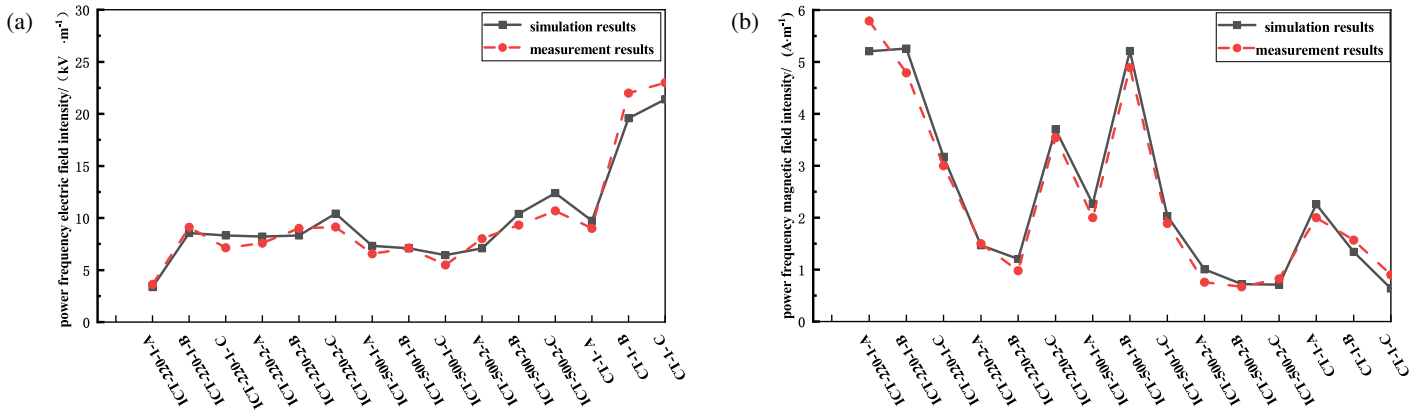

FIGURE 4. The verification of power frequency electromagnetic field: (a) power frequency electric field; (b) power frequency magnetic field.

the power frequency magnetic field must account for the angled arrangement of transmission lines. For a 110 kV power line, the line currents of the 110 kV transmission line range from 52,486.39 A to 262,431.9 A. Currents of 270 A with phases of 0°, 180°, 120°, 300°, 60°, and −120° are added to both ends of the 110 kV transmission line to simulate the power frequency magnetic field of the 110 kV transmission line. For a 220 kV power line, the line currents of the 220 kV transmission line range from 262.4319 A to 393.6479 A. Currents of 400 A with phases of 0°, 180°, 120°, 300°, 60°, and −120° are added to both ends of the 220 kV transmission line to simulate the power frequency magnetic field of the 220 kV transmission line. For a 500 kV power line, the line currents range from 692.8203 A to 1,154.701 A. Currents of 1,200 A with phases of 0°, 180°, 120°, 300°, 60°, and −120° are added to the 500 kV transmission line to simulate the power frequency magnetic field of the 500 kV transmission line [13]. This helps to some extent in ensuring the safety and stability of the system, making the simulation results more realistic and effective.

During on-site measurements, the field team used the SEM-600/LE-01 electromagnetic radiation analyzer with an electromagnetic field (EMF) probe to monitor power frequency electromagnetic emissions from the substation. The probe was positioned 1.5 meters above ground (simulating human exposure height) while operators maintained a 3-meter distance to avoid interference. The reliability of the model was validated through comparative analysis between simulation results and on-site measurement data, with detailed comparison outcomes presented in Figure 4.

As illustrated in Figure 4, the measured power frequency electric field values in the substation exhibit strong agreement with the simulated results, with closely aligned variation trends. The maximum deviation between measured and simulated power frequency electric fields occurs near the No. 2 500 kV interconnecting transformer (ICT-500-2). At this location, the measured value reaches 10.68 kV/m compared to the simulated 12.391 kV/m, yielding a peak relative error of 9.36%. The maximum deviation between measured and simulated power frequency magnetic fields occurs near the No. 1 220 kV interconnecting transformer (ICT-220-1). At this location, the measured magnetic flux density reaches 5.789 A/m compared to the simulated value of 5.2076 A/m, resulting in a peak relative error of 10.043% for the simulation. The observed discrepancies primarily stem from the modeling approach focusing on transmission line dominance while omitting secondary electrical equipment and non-critical metallic

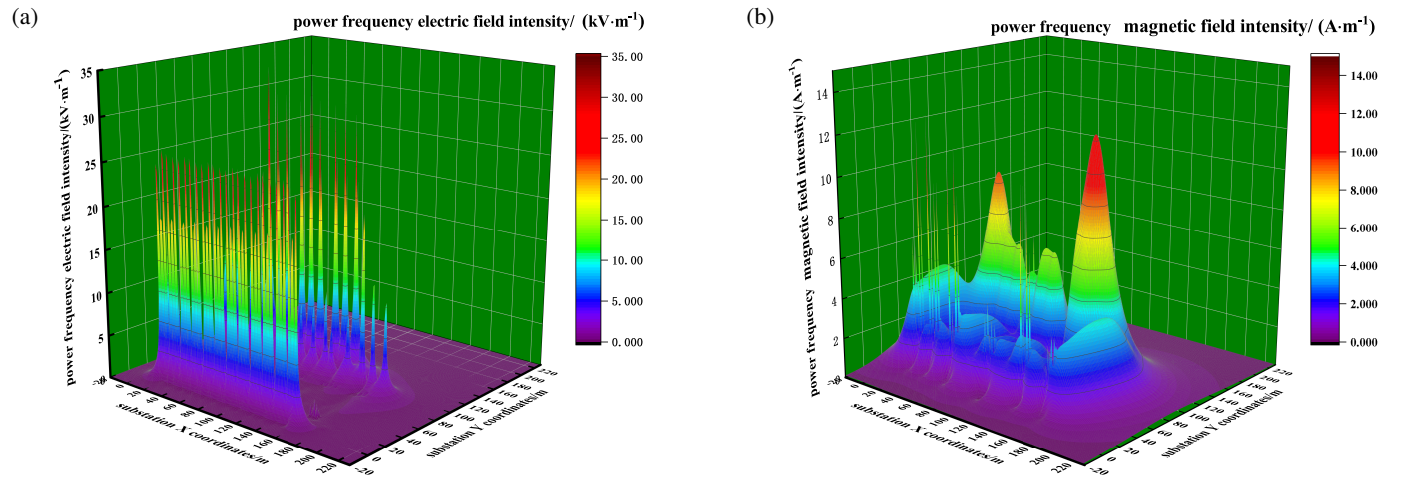

FIGURE 5. Power frequency electromagnetic field distribution at a height of 1.5 m above the ground: (a) power frequency electric field; (b) power frequency electric field.

structures with negligible influence on spatial power frequency electromagnetic fields. This deliberate simplification maintains computational efficiency while ensuring that the simulation error remains within 15%. Therefore, the electromagnetic field model of this transmission line is validated as effective.

The detection probe used for the power frequency electromagnetic field detection has a height of 1.5 m, and the personnel are positioned 3 m away from the probe. Therefore, an analysis of the power frequency electromagnetic field distribution of the transmission lines at a height of 1.5 m above the ground was conducted. The power frequency electromagnetic field distribution at a height of 1.5 m above the ground is shown in Figure 5.

As shown in Figure 5, there are significant variations in both electric field intensity and magnetic field intensity across different spatial regions. The maximum power frequency electric field intensity in the substation was measured at 30.893 kV/m, occurring at the No. 1 500 kV interconnecting transformer (ICT-500-1), while the peak magnetic field intensity reached 10.55 A/m at the No. 3 500 kV interconnecting transformer (ICT-500-3). The measured maximum values of both power frequency electric field (30.893 kV/m) and magnetic field (10.55 A/m) significantly exceed the national standard limits of 10 kV/m and 3 A/m, respectively. This indicates that electromagnetic field radiation intensities in certain areas of the substation have reached or surpassed the regulatory thresholds, potentially posing risks to surrounding environments and equipment. Therefore, it is imperative to conduct further research on the impact of power frequency electromagnetic fields from substation transmission lines on 5G base stations, ensuring their normal operation.

4. MUTUAL INTERFERENCE ANALYSIS

The deployment of 5G communication base stations within substations, including the installation of base station antennas and communication equipment rooms, enables high bandwidth, low latency, and widespread connectivity. This advancement elevates real-time communication within the substation to an unprecedented level. The electromagnetic interference from 5G base station antennas to secondary equipment in substations primarily originates from radio frequency (RF) radiation. Under normal operating conditions, although there is no direct conductive connection between base station antennas and secondary equipment, the antennas continuously emit time-varying high-frequency electromagnetic waves during operation. This inevitably generates radiated electromagnetic disturbances to secondary equipment within the radiation range. In addition, in the complex electromagnetic environment of the substation, there is spectral overlap between the operating frequency band of the 5G receiving antenna and the electromagnetic interference signals from the secondary equipment. This spectral overlap may result in a decrease in the reception efficiency of the 5G base station antenna. Therefore, when arranging communication equipment within the station, it is necessary to consider whether 5G communication equipment has an impact on the secondary equipment within the station. By implementing proper planning and design, it is possible to achieve effective coordination between 5G communication equipment and secondary equipment within the station.

To study the impact of 5G communication equipment on secondary devices, reference is made to the relevant provisions of YDT 2583.17–2019 (Electromagnetic Compatibility Requirements and Test Methods for Cellular Mobile Communication Equipment). This standard stipulates an immunity threshold of 3 V/m for equipment exposed to RF radiation in the 80–690 MHz range. For the 690–6000 MHz range, the threshold is 10 V/m (electric field) and 3 A/m (magnetic field).

The allocation of 5G frequency bands is based on specific frequency ranges, which are categorized into distinct bands. Each band possesses unique characteristics and application scenarios. The 5G frequency ranges adopted by various telecommunications operators are detailed in Table 2.

Among them, 700 MHz (n28), 900 MHz (n8), 1800 MHz (n3), 2600 MHz (n41), 3500 MHz (n78), and 4900 MHz (n79) are the mainstream frequency bands of 5G in China [14].

TABLE 2. 5G frequency bands ranges for each telecommunication operator.

telecommunication operator	telecommunication operator	ranges (MHZ)
China Mobile	n41	2515–2675
	n79	4800–4900
China Telecom	n5	825–835/870–880
	n1	1920–1940/2110–2130
	n78	3400–3500
China Unicom	n8	904–915/949–960
	n1	904–915/949–960
	n3	1710–1785/1805–1880
	n78	3500–3600
China Broadcasting Network	n28	703–733/758–788
	n79	4900–4960

TABLE 3. The maximum electric field values in the area of the secondary equipment.

5G operating frequency/MHZ	the peak value of an electric field/ ($V \cdot m^{-1}$)	the peak value of a magnetic field/($mA \cdot m^{-1}$)
700	1.1	3
900	4	9.9
1800	7.59	18.06
2600	7.73	20.28
3500	9.69	25.89
4900	10.55	27.90

4.1. 5G Communication Equipment Impact on Substation Secondary Equipment

To study the impact of 5G communication equipment on the secondary equipment inside the substation, we established a simulation model of the 5G communication equipment. The transmitting power range of 5G base station antennas currently deployed in substations is 15–200 W. The 5G base station antenna is typically positioned tens to hundreds of meters away from the equipment area. Therefore, a 5G communication device radiation model has been deployed at the center of the substation's transmission lines, specifically at coordinates (100, 100, 20). The antenna has a transmitting power of 200 W and a horizontal azimuth angle of 45°. This study focuses on mainstream 5G frequency bands to systematically investigate the potential electromagnetic interference effects of 5G communication equipment on secondary devices in substations. The currently deployed 5G base station antennas in smart substations have a maximum transmitting power of 200 W [15], which is sufficient to cover the majority of operational scenarios. Therefore, to simulate the most demanding physical conditions, the transmitting power of the antenna was set to 200 W, with a horizontal azimuth of 45° to maintain consistency and comparability in the simulation experiments. By maintaining the same power level, it is possible to more accurately compare the RF interference effects of different frequency bands and observe the RF interference situations under different frequency bands more clearly, thereby obtaining more reliable simulation results and conclusions. Through electromagnetic field simulations of substation secondary equipment areas under 5G band interference, the maximum electromagnetic field intensities in these zones were obtained, as summarized in Table 3.

When the operating frequency of the 5G communication equipment is 4900 MHz, the electromagnetic field intensity coupled to secondary equipment in the substation by the radiated signals from the 5G device is illustrated in Figure 6.

Based on Table 3 and Figure 6, it can be concluded that electromagnetic wave attenuation occurs during propagation in space, and the operating frequency of the 5G base station antenna exerts a measurable influence on the electromagnetic field intensity within the substation [16]. When the operating frequency of the 5G antenna is 700 MHz, 900 MHz, 1800 MHz, 2600 MHz, or 3500 MHz, the impact of 5G communication equipment on secondary devices within the substation is relatively minor. The electromagnetic field intensity coupled to the secondary equipment in these frequency bands remains below the standard thresholds of 10 V/m (for 690–6000 MHz) and 3 A/m (magnetic field). When the operating frequency of the 5G antenna is 4900 MHz, the electromagnetic signals radiated by 5G equipment within the substation induce maximum electric and magnetic field intensities at secondary equipment locations. The peak electric field reaches 10.55 V/m (exceeding the EMC immunity threshold of 10 V/m), while the peak magnetic field measures 27.90 mA/m. Therefore, when deploying 5G communication equipment, it is necessary to consider the electromagnetic interference of 5G communication equipment on secondary equipment within the substation. It is recommended

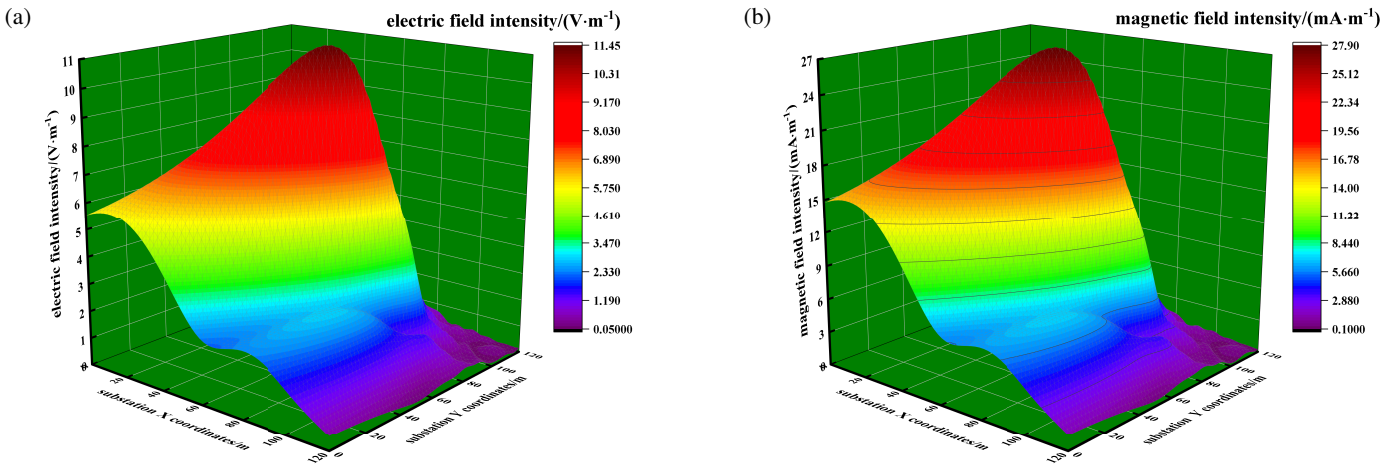

FIGURE 6. Electromagnetic field intensity distribution at 4900 MHZ in the secondary equipment area: (a) Electric field distribution; (b) Magnetic field distribution.

TABLE 4. The spatial electromagnetic field distribution of electromagnetic radiation sources inside the substation.

RF signal/MHZ	the peak value of an electric field/(mV·m^{-1})	the peak value of a magnetic field/(uA·m^{-1})
700	2250	5400
900	1150	4000
1800	2250	2768.5
2600	1125	3000
3500	3564	10800
4900	1500	4500

that when deploying 5G communication equipment inside the substation, measures such as adjusting the transmission power or azimuth angle of the base station antenna can be taken to ensure that the overall field strength within the station is less than 10 V/m.

4.2. The Impact of Secondary Equipment on 5G Communication Devices

To study the impact of secondary equipment on 5G communication devices, we established a simulation model of the secondary equipment inside the substation. Secondary equipment is typically housed in the main control room. By modeling the ground as an infinitely large perfect conductor, a rectangular cavity with a central window opening is used to simulate the substation's main control room. The rectangular cavity measures 15 meters in all three dimensions (length, width, height) and features a 2 m×2 m window, representing actual architectural window structures. A bar-type protective barrier is installed at the window opening to simulate ventilation ports and shielding mechanisms. A dual-dipole antenna device with a voltage excitation of 10 V is positioned at the central coordinate point of the main control room's spatial domain to simulate a standard electromagnetic emission source from secondary equipment [17]. Therefore, when the interference generated by secondary equipment is respectively at 700 MHz, 950 MHz, 1800 MHz, 2600 MHz, 3500 MHz, and 4900 MHz, considering the penetration loss of the main control room walls, the simulation analysis of the impact of secondary equipment in the substation on 5G communication equipment is shown in Table 4.

As shown in Table 4, the maximum electric field intensity in the secondary equipment area is 3564 mV/m, and the maximum magnetic field intensity is 10800 μA/m — both values are below the standard limits of 10 V/m (for 690–6000 MHz) and 3 A/m, indicating that the electromagnetic interference from substation secondary equipment has minimal impact on 5G communication devices. Among the tested frequencies, when secondary equipment generates interference at 3500 MHz, the electric and magnetic field intensities in the substation's secondary equipment area are relatively higher than other bands. However, these values remain below the specified thresholds (10 V/m for electric field, 3 A/m for magnetic field), confirming that the EMI impact on 5G communication devices is not significant. The electromagnetic field intensity distribution at 3500 MHz in the secondary equipment area is supported by simulation results in Figure 7 distribution at 3500 MHz.

In summary, within substation environments, secondary equipment exhibits minimal electromagnetic interference impact on 5G base station devices, confirming that 5G infrastructure can be safely deployed in substations. Although low-frequency and mid-frequency bands exhibit relatively higher electric and magnetic field intensities, these values remain significantly below regulatory thresholds (10 V/m for electric fields, 3 A/m for magnetic fields). Thus, secondary equipment emissions do not pose significant operational risks to 5G base stations.

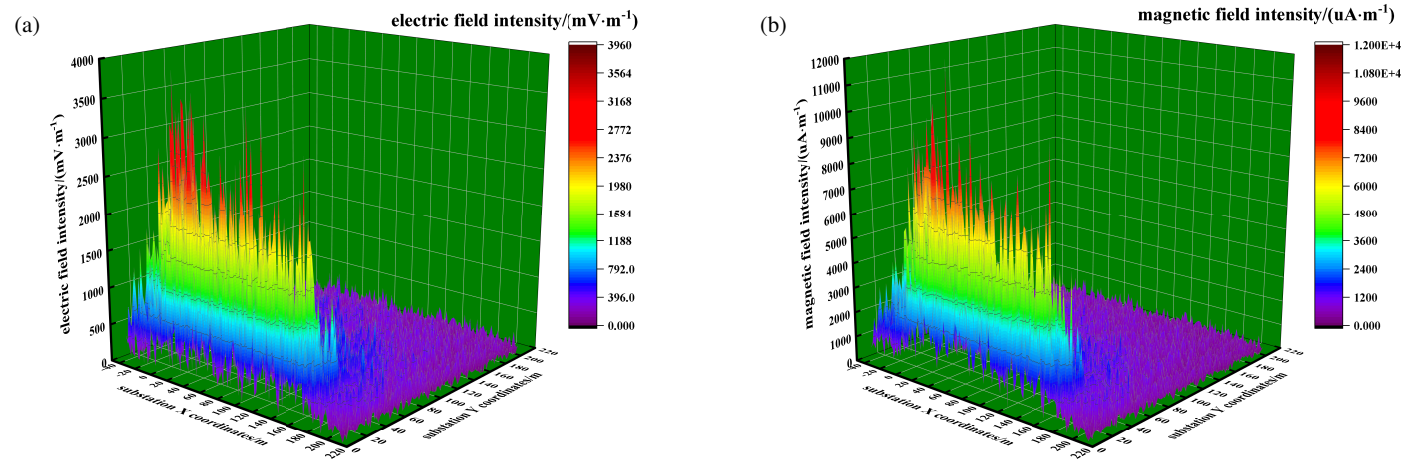

FIGURE 7. Electromagnetic field intensity distribution at 3500 MHz: (a) Electric field distribution; (b) Magnetic field distribution.

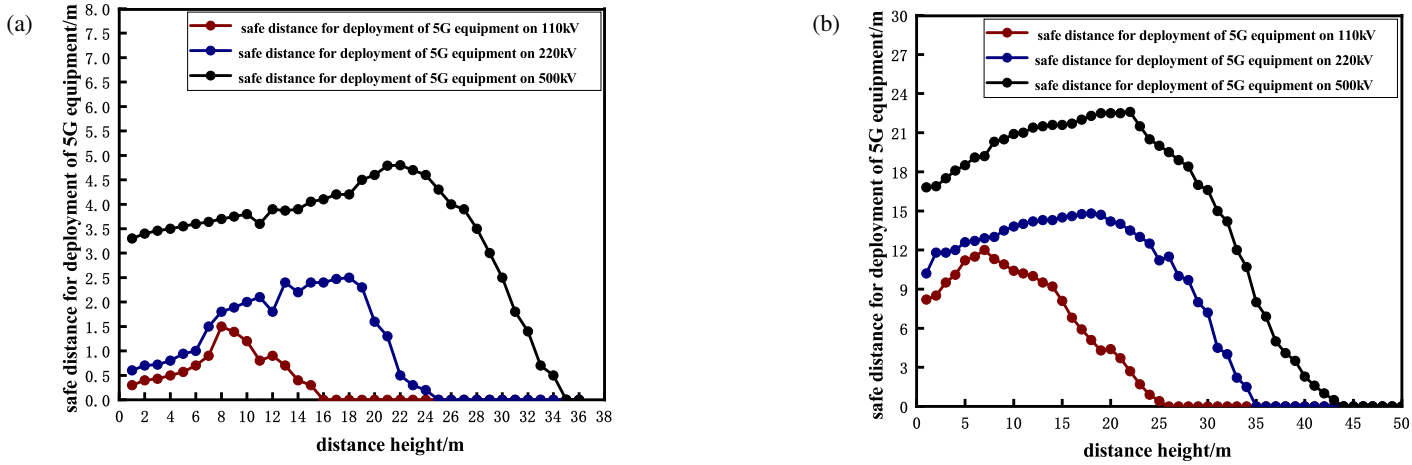

FIGURE 8. The safe range for the accurate deployment of 5G communication equipment at different heights: (a) power frequency electric field; (b) power frequency magnetic field.

5. IMPACT OF POWER FREQUENCY ELECTROMAGNETIC FIELDS

To ensure the long-term stable operation of 5G base stations within substations, continuous monitoring and mitigation of power frequency electromagnetic fields (50 Hz) are critical to safeguarding the reliability of 5G communication equipment [18]. Based on GBZ 17799.6–2017 (Electromagnetic Compatibility Generic Standards-Immunity for Power Plants and Substations) and YD/T 2583.17–2019 (Electromagnetic Compatibility Requirements and Test Methods for Cellular Mobile Communication Equipment-Part 17:5G Base Stations and Ancillary Devices), the national standard limits for electromagnetic fields in substations are defined as follows: the power frequency electric field shall not exceed 10 kV/m, and the power frequency magnetic field shall not exceed 3 A/m. In China, the installation height of most 5G communication antennas falls within the range of 2 to 50 meters, with rare exceptions reaching up to 120 meters. Therefore, based on the model of the power frequency electromagnetic field of the transmission line in the substation, simulations were carried out to calculate the intensity of the power frequency electromagnetic field within the range of 1–50 meters above the ground. By doing this, we can determine the safe deployment range for 5G communication devices at different heights above the ground.

According to standard configurations of high voltage overhead transmission lines in China: 110 kV lines are installed at approximately 8 meters above ground with a rated current of 270 A; 220 kV lines are elevated to about 18 meters, carrying 400 A; 500 kV lines reach 22 meters in height and conduct 1200 A. The safe deployment boundary for 5G communication equipment is defined as the radial area around the ground projection or spatial position of power transmission lines where the electromagnetic field intensity exceeds national standard limits. The specific results of the safe range for the accurate deployment of 5G communication equipment at different heights of the power frequency electromagnetic field of the substation transmission lines from the ground are shown in Figure 8.

According to Figure 8, the safe distance of 5G communication equipment exhibits an initial increase followed by a decrease as the height above ground increases. The safe distance reaches its maximum when the height matches the overhead line elevation corresponding to the voltage level. When the safe distance decreases to 0 meters, the electromagnetic compati-

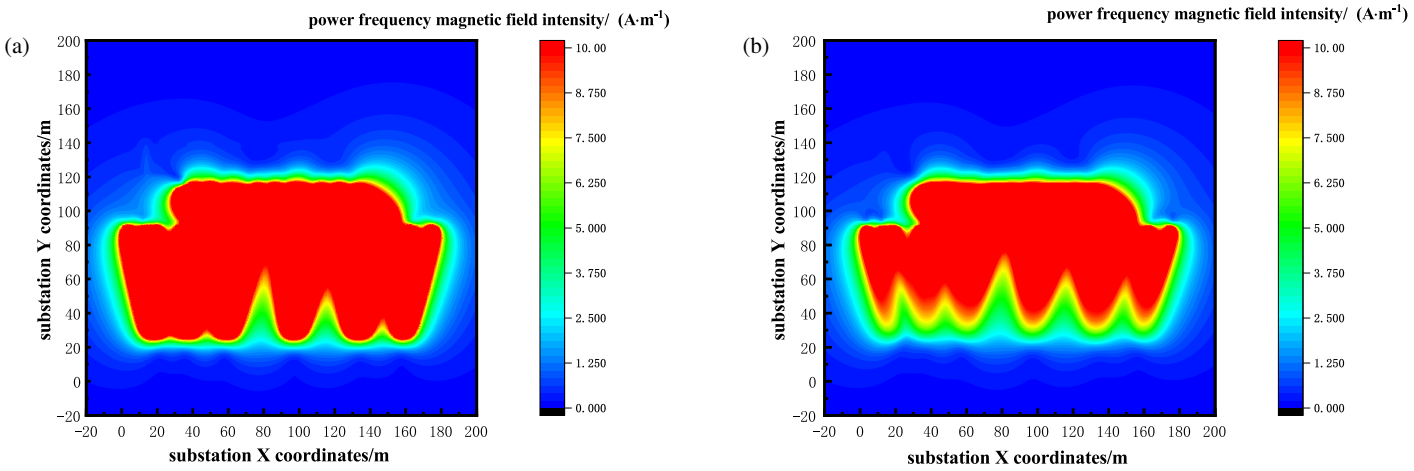

FIGURE 9. Magnetic field intensity at the height of overhead transmission lines: (a) Power frequency magnetic field intensity at height of 220 kV overhead lines; (b) Power frequency magnetic field intensity at height of 500 kV overhead lines.

bility meets the standard requirements, enabling unobstructed deployment across the entire planar space. A comparison between Figures 8(a) and 8(b) reveals that the safe deployment range of 5G equipment under power frequency magnetic fields is significantly larger than that under power frequency electric fields. This indicates that power frequency magnetic fields have a more substantial impact on 5G deployment than power frequency electric fields. When deploying 5G communication equipment, priority should be given to the impact of power frequency magnetic fields on 5G base station placement. As shown in Figure 8(b), within a ground-projection radius of 11.8 meters for 110 kV power lines, 13.9 meters for 220 kV lines, and 23.2 meters for 500 kV lines, the magnetic field intensity may exceed 3 A/m. Consequently, 5G communication devices cannot be deployed in these areas. Unobstructed full-plane coverage can only be achieved when the installation height exceeds 26 meters (for 110 kV lines), 35 meters (for 220 kV lines), or 46 meters (for 500 kV lines), respectively.

The power frequency magnetic field distribution at the height of overhead power lines is shown in Figure 9.

6. CONCLUSION

When deploying 5G communication equipment within substations, the primary consideration should be the long-term stability of power frequency magnetic field effects. This requires integrating the impact of 5G devices on secondary substation equipment, rationally planning deployment locations, and implementing shielding measures in high-risk zones. Such measures will effectively mitigate power frequency magnetic interference on 5G systems, ensuring stable cooperation between 5G networks and substation infrastructure. The specific deployment plan for 5G communication equipment in the complex electromagnetic environment within the substation is as follows:

(1) The operating frequency of 5G base station antennas can influence the field strength within substations. When 5G antenna operates at 4900 MHz, the electromagnetic signals radiated by 5G equipment induce peak electric and magnetic field coupling at secondary equipment locations, with a maximum electric field value of 10.55 V/m. This exceeds the electromagnetic compatibility immunity threshold of 10 V/m. Therefore, when deploying 5G communication equipment in substations, appropriate mitigation measures such as adjusting the antenna's transmit power or azimuth angle should be implemented to ensure that the overall field strength remains below 10 V/m.

(2) Within substations, electromagnetic interference from secondary equipment to 5G base station devices is negligible, allowing safe deployment of the 5G infrastructure. While electric and magnetic field intensities in low- and mid-frequency bands remain relatively higher, they still fall significantly below permissible thresholds. Thus, secondary equipment does not have a material impact on 5G base station performance.

(3) The impact of the power frequency magnetic field within the substation on the deployment of 5G equipment is significantly greater than the impact of the power frequency electric field on the deployment of 5G communication equipment. Therefore, when deploying 5G communication equipment, priority should be given to considering the impact of the power frequency magnetic field. Specifically, within a radius of 11.8 m around the ground projection of the 110 kV line, 13.9 m around the ground projection of the 220 kV line, and 23.2 m around the ground projection of the 500 kV line, the magnetic field intensity may exceed 3 A/m. Therefore, 5G communication equipment cannot be deployed in these areas. Achieving obstacle-free coverage across the entire plane is possible when the height above the ground is higher than 26 m, 35 m, and 46 m, respectively.

(4) This study primarily focuses on the impact of long-term stable power frequency electromagnetic fields within substations on 5G communication equipment, as well as the mutual interference between 5G devices operating in different frequency bands and secondary substation equipment. The effects of transient electromagnetic phenomena, such as electrical fast transients generated by switching operations and surge impulses caused by lightning strikes, on 5G deployment will be thoroughly analyzed in subsequent research.

REFERENCES

[1] Li, Y., S. Wang, B. Tang, L. Zhang, Z. Shang, and X. Liu, "Analysis of 5G channel loss and its influencing factors in substation based on ray tracing algorithm," *The Journal of Engineering*, Vol. 2023, No. 3, e12234, 2023.

[2] Yao, Y., C. Liu, D. Qi, Z. Zhu, and W. Zhang, "Location of 5G base station antenna in substation taking into account path loss and RF radiation," *Discover Applied Sciences*, Vol. 6, No. 11, 556, 2024.

[3] Li, W., A. Sun, X. Wang, Y. Chen, C. Wang, Y. Li, and C. Xia, "Isolated orthogonal magnetic energy harvesting system around high voltage transmission lines," *Journal of Electrical Engineering & Technology*, Vol. 19, No. 7, 4239–4252, 2024.

[4] Ge, S., W. Liu, X. Li, and D. Ding, "Coupling characteristics of electromagnetic disturbance of on-site electronic device power port in substations and its suppression," *IEEE Transactions on Electromagnetic Compatibility*, Vol. 63, No. 5, 1584–1592, 2021.

[5] Zhu, S., J. Li, X. Hu, and Y. Yi, "One-dimensional parallel forward modeling for geophysical electromagnetic fields excited by sagging overhead transmission lines," *Computers & Geosciences*, Vol. 185, 105542, 2024.

[6] Fu, Z., Y. Zhang, X. Zhao, F. Du, S. Geng, P. Qin, Z. Zhou, L. Zhang, and S. Chen, "An ANN-based channel modeling in 5G millimeter wave for a high-voltage substation," *IET Communications*, Vol. 15, No. 19, 2425–2438, 2021.

[7] Chen, W., G. Xue, W. Song, D. Hou, and Y. Wang, "Accurate calculation and characteristic analysis of power frequency electromagnetic field generated by AC high voltage transmission line," *Chinese Journal of Geophysics*, Vol. 65, No. 5, 1813–1821, 2022.

[8] Wei, Q., X. Ge, J. Liu, and H. Li, "A study on the ambient electromagnetic radiation level of 5G base stations in typical scenarios," *Radiation Detection Technology and Methods*, Vol. 8, No. 3, 1333–1341, 2024.

[9] Huang, C., W. Huang, H. Jiang, J. Li, X. Tian, *et al.*, "Research on transmission characteristics of 5G signal for indoor substation based on ray tracing," in *Journal of Physics: Conference Series*, Vol. 2384, No. 1, 012029, 2022.

[10] Chen, H. and Y. Chen, "Modeling and simulation analysis of power frequency electric field of UHV AC transmission line," *International Journal of Advanced Computer Science and Applications*, Vol. 6, No. 1, 2015.

[11] Mujezinovic, A., E. Turajlic, A. Alihodzic, N. Dautbasic, and M. M. Dedovic, "Novel method for magnetic flux density estimation in the vicinity of multi-circuit overhead transmission lines," *IEEE Access*, Vol. 10, 18 169–18 181, 2022.

[12] Titov, V. S., C. Downs, Z. Mikić, T. Török, J. A. Linker, and R. M. Caplan, "Regularized biot-savart laws for modeling magnetic flux ropes," *The Astrophysical Journal Letters*, Vol. 852, No. 2, L21, 2018.

[13] Niu, H. C., J.-Q. Fan, and T. H. Hou, "Influence of power frequency magnetic field interference in substation on 5G base station deployment," *Progress In Electromagnetics Research C*, Vol. 124, 1–10, 2022.

[14] Tikhomirov, A., E. Omelyanchuk, and A. Semenova, "Recommended 5G frequency bands evaluation," in *2018 Systems of Signals Generating and Processing in the Field of on Board Communications*, 1–5, Moscow, Russia, Mar. 2018.

[15] Qi, D., X. Xi, C. Zhang, B. Tang, and X. Liu, "Electromagnetic interference from 5G base station antenna in substation on secondary equipment," in *2021 IEEE 2nd China International Youth Conference on Electrical Engineering (CIYCEE)*, 1–7, Chengdu, China, Dec. 2021.

[16] Hua, Q., Y. Huang, A. Alieldin, C. Song, T. Jia, and X. Zhu, "A dual-band dual-polarized base station antenna using a novel feeding structure for 5G communications," *IEEE Access*, Vol. 8, 63 710–63 717, 2020.

[17] Yazdani, R., H. Aliakbarian, A. Sahraei, and G. A. E. Vandenbosch, "A compact triple-band dipole array antenna for selected sub 1 GHz, 5G and WiFi access point applications," *IET Microwaves, Antennas & Propagation*, Vol. 15, No. 15, 1866–1876, 2021.

[18] Wang, X., Y. Nie, Z. Li, and H. Qiu, "Analysis of cable path location and its influencing factors based on power frequency magnetic field," *Journal of Electric Power Science and Technology*, Vol. 38, No. 2, 96–104, 2023.